Analysis of the multilayer organization of a sunflower leaf during dehydration with terahertz time-domain spectroscopy

Yannick Abautret, Dominique Coquillat, Michel Lequime, Myriam Zerrad, Claude Amra

Research Article | Vol. 30, No. 21 / 10 Oct 2022 / Optics Express 37971
Optics EXPRESS

Analysis of the multilayer organization of a sunflower leaf during dehydration with terahertz time-domain spectroscopy

YANNICK ABAUTRET,[1,*] DOMINIQUE COQUILLAT,[2] MICHEL LEQUIME,[1] MYRIAM ZERRAD,[1] AND CLAUDE AMRA[1]

[1]Aix Marseille Univ., CNRS, Centrale Marseille, Institut Fresnel, Faculté des Sciences - Campus Saint Jérôme, Avenue Escadrille Normandie-Niemen, 13397 Marseille, France
[2]Laboratoire Charles Coulomb (L2C), Université de Montpellier, CNRS, Montpellier, France
*yannick.abautret@fresnel.fr

Abstract: We apply reverse engineering techniques (RET) to analyze the dehydration process of a sunflower leaf with terahertz time-domain spectroscopy. The multilayer structure of the leaf is extracted with accuracy during the entire process. Time variations of thickness and the complex index are emphasized for all leaf layers (2 cuticules, 2 epiderms, and 2 mesophylls). The global thickness of the sunflower leaf is reduced by up to 40% of its initial value.

1. Introduction

Global warming and climate changings are inducing multiple violent phenomenon such as proliferation of drought area. In this hostile context to agricultural production, it is important to know and understand better physiologic mechanisms of plants. More precisely, it will be necessary to deal smartly with water resources depending on plants behavior facing water stress in order to keep a yield production as high as possible. For several decades, precision farming has been a domain that tries to find out how to probe and control, in an optical non-intrusive way, the plants physiologic parameters of interest.

Over the past decades, numerous non-contact techniques have been developed to understand plant behavior facing biotic and abiotic stresses. The general idea is to offer agronomists new non-destructive tools which allow them to improve variety selection or to accurately estimate physiologic status of plants [1,2]. Optical techniques have been largely used and most often rely on luminescence [3], hyperspectral imaging [4] or statistical study of speckle patterns [5,6]. Also, terahertz (THz) metrology [7–9] has shown great interest to monitor water status in plants [10–12].

Despite the major role of these techniques for plant investigation, few knowledge was revealed about the internal organization of leaves with these non-contact techniques. Indeed most information is global or physico-chemical in nature, and does not emphasize the leaf multilayer structure which may gather several sub-layers in its depth (see Fig. 1(a)). To solve this issue we recently showed [13] how this multilayer structure could be analyzed in detail by reverse engineering techniques (RET) applied on time-domain spectroscopy (TDS) data. RET have been extensively used in optics to analyze the design of optical interference coatings [14] with thicknesses around a visible wavelength (i.e. a fraction of micrometer). However they could not be applied to the optical analysis of leaf structure, due to strong inhomogeneities in the leaves which scatter the whole incident light into a complex speckle pattern. Hence the basic idea of [13] was to extrapolate these techniques to the THz regime which involves much greater wavelengths (by 3 decades) than those of the visible regime. Because scattering is known to decrease at large wavelengths, the strong scattering reduction in the THz regime makes the leaf's

#463228 https://doi.org/10.1364/OE.463228
Journal © 2022 Received 10 May 2022; revised 29 Jul 2022; accepted 3 Aug 2022; published 29 Sep 2022

Optics EXPRESS

structure to appear as a homogeneous multilayer (see Fig. 1(b)) which reflects, transmits and absorbs almost the entirety of the incident light.

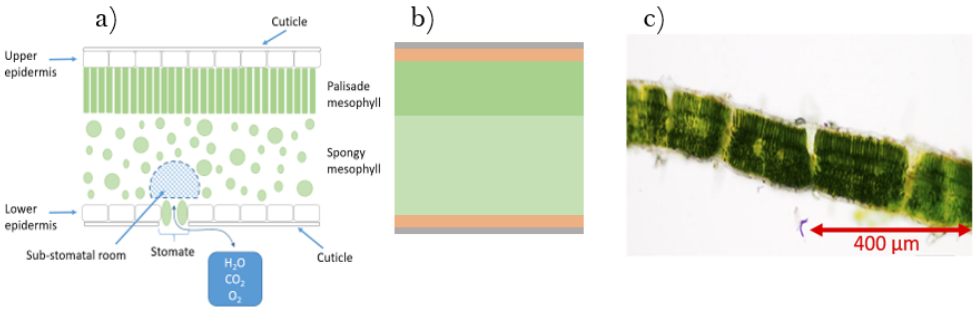

Fig. 1. (a) Schematic draft of a plant leaf, (b) THz wave sees the leaf as a homogeneous multilayer, and (c) cross-section of a leaf observed with optical microscopy.

Under these conditions the THz specular response of the leaf carries information on its depth organization at the THz scale, which can be retrieved with RET. The accuracy on the multilayer structure (thicknesses and complex indices) increases with the width of the spectral range, provided that index dispersion is moderate. Beyond the experimental aspects, it is important to point out some key differences between the optical and THz RET. One major difference is that the optical technique relies on spectrophotometric measurements in a continuous regime (i.e. intensity data are recorded at each wavelength), while the TDS technique involves a pulsed pico-second source (i.e. we record the time-response of the amplitude signal). Hence though the two techniques lead to identical results (due to the time-frequency equivalence), the TDS technique provides more information (modulus and phase quantities in the Fourier plane) than the optical one (modulus quantity).

Our recent results [13] have proved the relevance of the TDS technique. A 8-layer structure was revealed for a sunflower leaf, with the detail of thicknesses and complex indices. This multilayer structure has led to high agreement between calculated and measured data in the time or frequency domains. As often in reverse engineering, a few questions may remain about the unicity of the solution, especially since dispersion was neglected in the spectral range (100 GHz to 1 THz).

However the resulting leaf organization is similar to what can be expected in the literature (Fig. 1(a)).

Relying on these successful results, we here apply the TDS technique to investigate the temporal dehydration process of a sunflower leaf, which is the purpose of this work. Actually the plant behavior under dehydration could bring new information about how plant leaves face water stress over a prolonged period. Hence the multilayer structure of a leaf was analyzed every 12 mn during 16 hours after it has been separated from the plant. Every 12 mn the multilayer structure was analyzed, and this emphasizes shrinkage of the different layers so as to face water stress until a critical point, before the structure collapses because of strong dehydration.

The paper is organized as follows. Section 2 is first devoted to improvements in the reverse engineering technique, namely to take into account the global leaf shrinkage versus time, which is responsible for a slight difference in the positions of the reference and the sunflower samples. In section 3, the experimental procedure is described and we gather all experimental data. Section 4 is devoted to reverse engineering on the dehydration data, while section 5 is for the conclusion.

Optics EXPRESS

2. Improvement and adjustment of RET algorithm during dehydration process

2.1. Taking account of the global sheet shrinkage during dehydration

As already stressed, the shrinkage of the leaf modifies its position on the sample holder during dehydration, and this may create a phase shift which alters the data interpretation. In this section we analyze this process and show how to solve this difficulty. Actually the measurements in reflection mode require to register two signals in time domain. The first signal is for the reference $s_{ref}(t)$, that is, the reflection of the incident THz pulse on a gold mirror. The second signal $s(t)$ is for the reflection by the leaf sample of the same incident field. These two signals are then compared in the frequency domain by a ratio that defines the transfer function $\hat{H}(f)$ as:

$$\hat{H}(f) = \frac{FT[s(t)]}{FT[s_{ref}(t)]} = \frac{\hat{s}(f)}{\hat{s}_{ref}(f)} \tag{1}$$

where Fourier transform (FT) indicates a Fourier transform versus time. Now with $\hat{e}(f)$ the spectrum of the incident THz pulse, $\hat{r}_{gold}(f)$ and $\hat{r}(f)$ the reflection coefficients of the gold mirror and of the sunflower sample, we can write in the Fourier domain:

$$\hat{s}_{ref}(f) = \hat{e}(f)e^{i\varphi_1}e^{i\varphi_2}\hat{r}_{gold}(f) \tag{2}$$

$$\hat{s}(f) = \hat{e}(f)e^{i\varphi_1}e^{i\varphi_2}\hat{r}(f) \tag{3}$$

In these relations φ_1 and φ_2 are phase terms which characterize the paths l_1 and l_2 illustrated in Fig. 2(c). At this step the gold mirror is considered ideal so that its reflection is written as $\hat{r}_{gold}(f) = -1$. Hence the transfer function can be identified to the reflection coefficient of the sample as:

$$\hat{H}(f) = -\hat{r}(f) \tag{4}$$

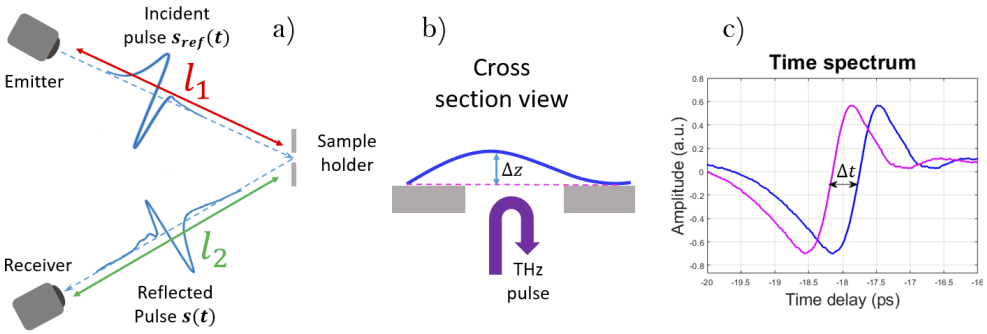

Fig. 2. (a) Illustration of the path lengths of incident (l_1) and reflected (l_2) fields. (b) Global leaf shrinkage with an average shift value Δz, which is responsible for a shift Δt in the temporal response (c).

Now we must stress on the fact that the paths l_1 and l_2 may be different for the reference and leaf samples. Indeed an offset position Δz may occur (Fig. 2(b)) between the reference mirror and the leaf sample, due to the poor leaf flatness. Furthermore this offset may vary with time during the dehydration process, because of leaf shrinkage shift. If we introduce the position offset Δz in equations (1-4), the transfer function becomes:

$$\hat{H}(f) = -\hat{r}(f)e^{i\varphi(\Delta z)} \quad \text{with} \quad \varphi(\Delta z) = 4\pi f\frac{\Delta z}{c} \tag{5}$$

Relation (5) shows that the transfer function that we measure is different from the reflection coefficient of the sample to analyze. In the Fourier domain, the phase of the sample reflection

Optics EXPRESS

would be linearly shifted in frequency. Note also that the offset Δz can be positive or negative. To summarize, in regard to the thickness-to-wavelength ratios involved in the experiment, the impact of Δz must be considered with accuracy because it can be confused with a particular leaf layer of thickness Δz. And this is all the more important as the Δz offset varies with time, due to the dehydration process.

The solution that we propose consists in adding a supplementary layer in the reverse engineering algorithm. This layer is an air layer of thickness Δz on the illumination side of the leaf. Hence it participates in the multilayer structure of the leaf, so that the reflection coefficient of the stack consisting of the leaf and the offset layer is $\hat{r}_s(f)e^{i\varphi(\Delta z)}$. With this procedure we will see that an excellent agreement is reached between theory and experiment. Eventually once all stack parameters have been determined (including Δz), it is immediate to remove the air layer which can be identified by its refractive index and its position (on the illumination side).

The results obtained with this modified algorithm are shown in Fig. 3. Recall that the algorithm measures a distance between the measured and calculated spectra, and uses a merit function for each given layer number N. Once the merit function reaches its minimum value with N, the multilayer solution is hold. With the sunflower leaf sample, the best solution was reached with a 7-layer stack, that is, a 6-layer leaf and an offset layer. The merit function is stationary for greater N values. As can be seen in Fig. 3 (left and center), the agreement is high in both the time and frequency domains. The spectral range is $200\,GHz - 1.2\,THz$, with a frequency step of $1\,GHz$. The temporal signal is analyzed over $1020\,ps$, with a time resolution of $0.02\,ps$. The number of data points is $M = 51000$ in both the time and Fourier domains. The offset layer is evaluated as $\Delta z = 60\,\mu m$, while the 18 leaf parameters are displayed in the right figure. The leaf structure is quasi-symmetric as expected, and includes 2 cuticules, 2 epidermis, and 2 mesophyll layers.

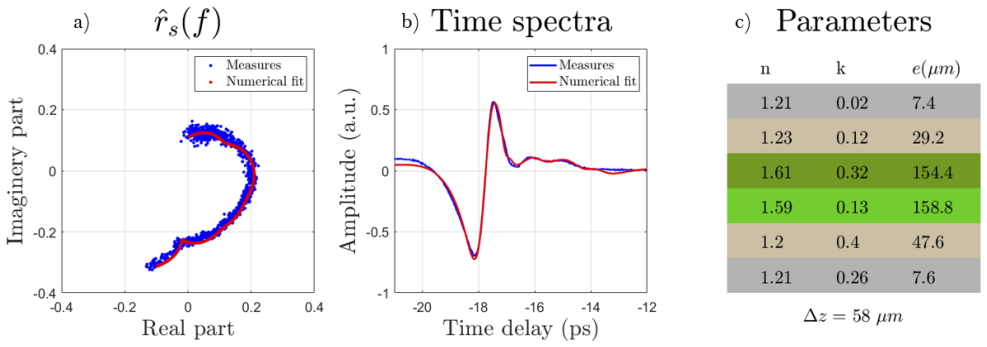

Fig. 3. Calculated (red curve) and measured (blue curve) TDS leaf signal in the Fourier (a) and (b) time domain. The leaf parameters are displayed in (c), with e the thickness, and $n + jk$ the complex refractive index.

It must be stressed here that we do not measure trichome layers as was done in a former work [13]. Actually these trichome layers have a refractive index close to unity, which is quasi-identical to that of the offset (air) layer. Hence the accuracy on these layers is very poor and this may explain why the merit function is stationary starting at 6 layers. This is not penalizing insofar as these layers have slight impact on the leaf spectrum.

To go further in this study, it is now interesting to test and use the new minimization procedure (with a 6-layer model plus an offset layer) over the whole measurements campaign we performed during dehydration process.

Optics EXPRESS

2.2. Precisions on RET algorithm

Here we summarize the main steps of the RET we applied to estimate the optical structure of the vegetal tissue. We recall here that we record time domain spectrum whereas we performed a numerical fit in frequency domain. This implies that the raw data are first projected into the Fourier space and then compared to the model. The different steps of the procedure are illustrated in Fig. 4 as follow:

- Measurement of the reference signal $s_{ref}(t)$;
- Measurement of the reference signal in reflection $s(t)$;
- Calculation of Fourier transform $\hat{s}_{ref}(f)$ and $\hat{s}(f)$;
- Calculation of the transfer function in reflection $\hat{H} = \hat{s}(f)/\hat{s}_{ref}(f)$;
- p-layers modelization X_p and construction of the reflection complex coefficient $\Gamma_R(X_p,f)$ relying on the admittance formalism [15];
- Formation of the merit function $M = |\hat{H}_R(f) - \Gamma_R(X_p,f)|$;
- Estimation of the structure by minimization of the merit function $\tilde{X}_p = \underset{X_p}{min}(M)$.

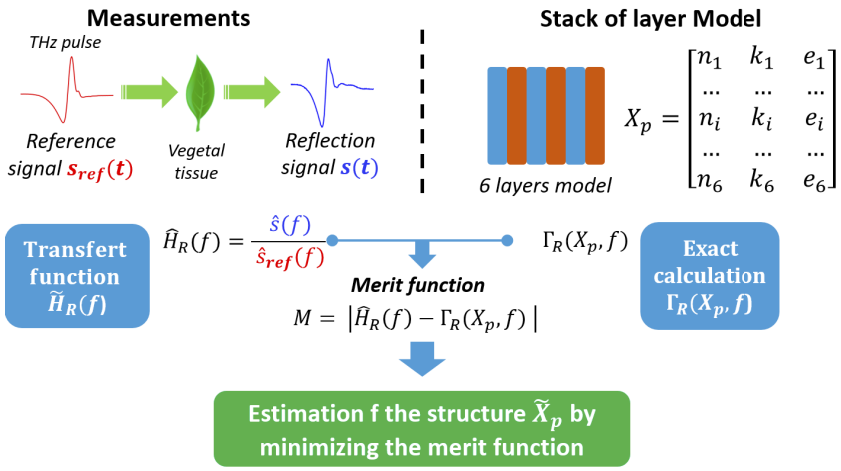

Fig. 4. Draft of the numerical treatment of the time domain spectra in order to estimate the inner physiologic organization of the sunflower leaf.

It should be here emphasized that the model we use relies on a stack of 6 homogeneous layers. This number of layers is considered fixed in this study. About the algorithm, we imposed specific constraints during minimization of the merit function. They are related to the bounderies of the differents opto-geometrical parameters that we are interested in. More precisely, we fixed:

- Refractive index $1 \leq n \leq 4$;
- Extinction coefficient $0 \leq k \leq 1$;
- Thickness (e).

Finally, we specify that the minimization algorithm exploits interior point method which is available on software. Each minimizing procedure uses about a hundred of iterations to converge that represents only few seconds.

Optics EXPRESS

Layers	min (μm)	max (μm)
Cuticule	0	15
Epidermis	10	50
Palisade M.	50	200
Spongy M.	0	200

3. Measurement campaign during dehydration process

The raw data in reflection we used to rebuild the internal leaf structure is taken from a series of 80 measurements which have been acquired successively. In this experiment, time spectra at the ps scale were acquired with Teraview TDS spectrometer in collaboration with Charles Coulomb laboratory (Montpellier, France). The vegetal material was developed and provided by INNOLEA (Mondonville) as a part of OptiPAG ANR project. Every time acquisition lasts around 12 minutes on the same leaf sample. In this case, time sampling is equal to time acquisition. This sample is a square peace of a vegetal tissue cut out from a fresh sunflower leaf (see Fig. 5). It has been fixed with some tape on a circular holder which allows light to pass through the tissue. In this configuration, the sample has no access to water resources anymore.

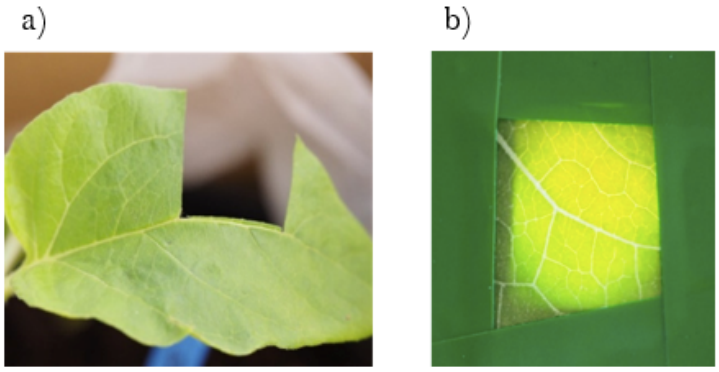

Fig. 5. (a) Leaf sample procedure and (b) holder.

Each time spectrum is the result of 100 scans which last thousand picoseconds. The frequency spectrum ranges from 200 GHz to 1200 GHz, with a resolution of 1 GHz. We recorded 80 time spectra in reflection mode every 12 minutes, so that the experiment lasted about 16 hours. The video shows simultaneously the evolution of the time and frequency spectra that have been acquired during this dehydration process (see Visualization 1).

We first observe that the time and Fourier signals present a time evolution with no "break". This means that data progression looks continuous for both of them and all over the dehydration process. Secondly, we notice that the double hump echoes in the time domain (which characterize the initial leaf time spectrum) are moving to the left until they are absorbed by the first echo as we can see in Fig. 6.

The fact that these echoes are getting closer in time means that the internal layer structure is shrinking during dehydration. Eventually, it is remarkable that the frequency spectrum which roughly draws number "3" at the beginning is moving slowly towards a well-known spiral curve that can be associated with the spectral response of a single layer absorbing plate. From these observations, it seems like, at first order approximation, the leaf internal structure basically

Optics EXPRESS

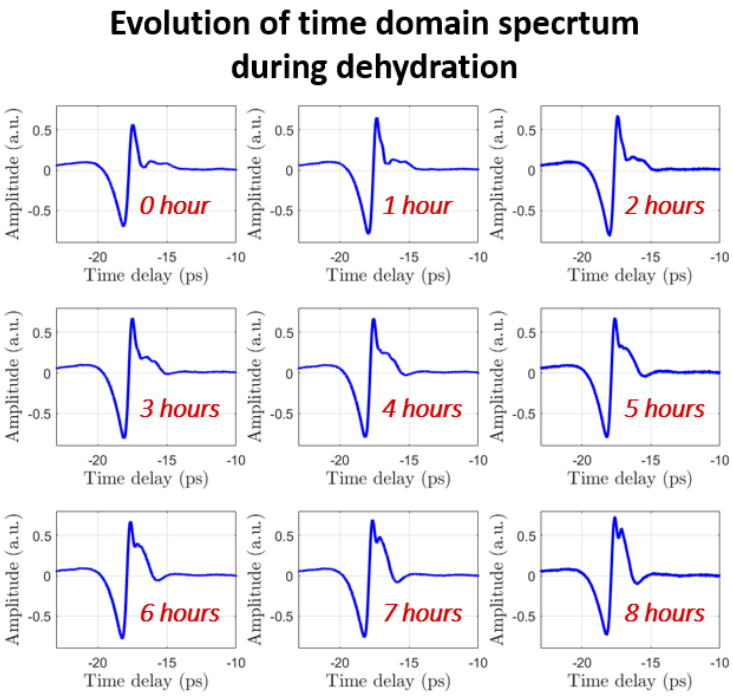

Fig. 6. Evolution of the reflected time domain spectra of the leaf during dehydration process from 0 to 8 hours (see Visualization 1).

reduces its total thickness when loosing water. This will be checked with accuracy in the next section.

4. Application of reverse engineering on dehydration data

We now apply the modified RET to these experiments. We considered the first 50 spectra among the 80 acquisitions that is, a total duration of 10 hours. For each acquisition the offset thickness was extracted, as well as the 18 leaf parameters which describe the leaf structure L_n at each instant $t_n = n * 12\,mn$.

In this multiple and successive minimization process we also add another constraint. It concern the continuity of the leaf structure from L_n to L_{n+1}. More exactly, the difference between the leaf parameters in structures L_n to L_{n+1} cannot exceed 10%. This hypothesis is rather intuitive and based on the fact that the internal leaf structure would not strongly change every 12 mn. Furthermore, the feeling of continuity that we noticed when looking at Visualization 1 is another element that argues in this way.

Working with this algorithm, we obtained the results presented in Visualization 2 which concern the first 50 acquisitions in the time domain. This corresponds to a 10 hours period of dehydration. The first structure is that of Fig. 3. Visualization 2 displays in red both the fit in the time domain (left) and in the frequency domain (right) for a frequency range of $[200GHz, 1200GHz]$. Measurements are in blue and show high agreement with the calculation at every instant t_n.

From these data we plotted in Fig. 7 the evolution of all opto-geometrical parameters during dehydration process. Results are presented by physical properties, that is to say, real refractive index (a), imaginary index (b), and thickness (c). Each couple of physical layers (cuticles,

Optics EXPRESS

epidermis, and mesophyl) are gathered under the same color. The time index variations can be seen for each layer. About the thicknesses, the highest variations appear for the mesophyll layers. Actually the thicknesses of these two layers look to regularly shrink until 40% percent of their initial value. This makes sense since we know that most of water contained in a leaf is mainly located in mesophyll; dehydration process implies the complete loss of water in the leaf, and this is translated by an important reduction of palisade and spongy mesophyll. On the other hand, cuticle and epidermis are hydrophobic protection layers which do not contain water, or very few, and we do not expect them to change their own physical structure when facing water stress. Thus, all result show that, when facing drought condition, the leaf internal structure is first impacted by the thickness reduction of its two mesophyll layers. This slimming process goes with loss of water and probably with destruction of cells and micro-structure.

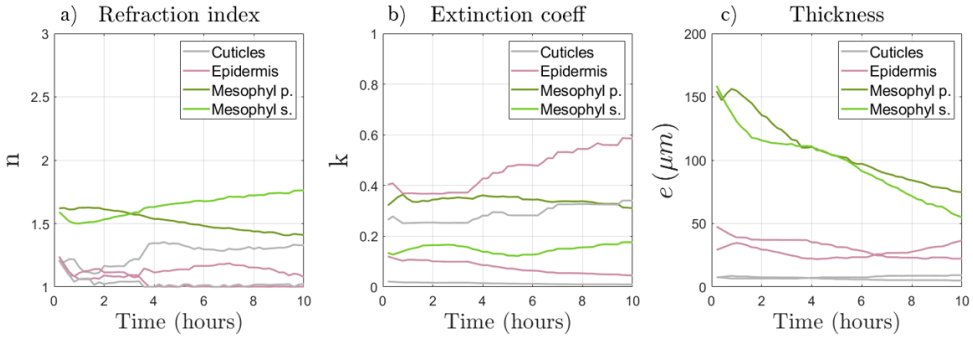

Fig. 7. (a) Time variation of real index, (b) imaginary index, and (c) thickness, for each leaf layer. Evolution in time of the fitting curves and thicknesses are presented in Visualization 2.

5. Conclusion

Taking into account the offset layer has led to excellent agreement between theory and experiment during the whole dehydration process, in both the time and Fourier domains. With this modification in the RET algorithm, the multilayer leaf structure can be extracted in a few seconds. Time variations of thickness and complex index were emphasized for all leaf layers (2 cuticules, 2 epiderms, and 2 mesophyl). The sunflower leaf was shown to reduce its global thickness up to 40% of its initial value during the process (10 hours).

All results appear to be consistent, so that the terahertz TDS technique provides a relevant non-destructive tool to analyze the internal opto-geometric organization of vegetal leaves. It may surely help in the investigation of biotic and abiotic stresses, for a variety of vegetal tissues.

Future work will complete the THz data with transmission data. This will give access to the absorption spectra of the leaves, a useful quantity to check the unicity of solutions.

Funding. Agence Nationale de la Recherche (ANR-16-CE04-0010).

Acknowledgments. This work was conducted within the OPTIPAG Project supported by the grant ANR-16-CE04-0010 from the French National Research Agency and by the Montpellier University of Excellence I-Site MUSE (PRIME@MUSE), the Région Occitanie, and by the "Gepeto Terahertz platform".

Disclosures. The authors declare no conflicts of interest.

Data availability. Data underlying the results presented in this paper are not publicly available at this time but may be obtained from the authors upon reasonable request.

References

1. A. Atefi, Y. Ge, S. Pitla, and J. Schnable, "Robotic Technologies for High-Throughput Plant Phenotyping: Contemporary Reviews and Future Perspectives," Front. Plant Sci. **12**, 611940 (2021).

Optics EXPRESS

2. Q. Qiu, N. Sun, H. Bai, N. Wang, Z. Fan, Y. Wang, Z. Meng, B. Li, and Y. Cong, "Field-Based High-Throughput Phenotyping for Maize Plant Using 3D LiDAR Point Cloud Generated With a Phenomobile," Front. Plant Sci. **10**, 554 (2019).
3. M. L. Pérez-Bueno, M. Pineda, and M. Barín, "Phenotyping Plant Responses to Biotic Stress by Chlorophyll Fluorescence Imaging," Front. Plant Sci. **10**, 1135 (2019).
4. H. Liu, B. Bruning, T. Garnett, and B. Berger, "Hyperspectral imaging and 3D technologies for plant phenotyping: From satellite to close-range sensing," Comput. Electron. Agric. **175**, 105621 (2020).
5. D. Héran, M. Ryckewaert, Y. Abautret, M. Zerrad, C. Amra, and R. Bendoula, "Combining light polarization and speckle measurements with multivariate analysis to predict bulk optical properties of turbid media," Appl. Opt. **58**(30), 8247 (2019).
6. M. Ryckewaert, D. Héran, E. Faur, P. George, B. Grözes-Besset, F. Chazallet, Y. Abautret, M. Zerrad, C. Amra, and R. Bendoula, "A New Optical Sensor Based on Laser Speckle and Chemometrics for Precision Agriculture: Application to Sunflower Plant-Breeding," Sensors **20**(16), 4652 (2020).
7. W. Lai, H. Cao, J. Yang, G. Deng, Z. Yin, Q. Zhang, B. Pelaz, and P. del Pino, "Antireflection self-reference method based on ultrathin metallic nanofilms for improving terahertz reflection spectroscopy," Opt. Express **26**(15), 19470 (2018).
8. M. E. Khani and M. H. Arbab, "Translation-Invariant Zero-Phase Wavelet Methods for Feature Extraction in Terahertz Time-Domain Spectroscopy," Sensors **22**(6), 2305 (2022).
9. N. Klokkou, J. Gorecki, J. S. Wilkinson, and V. Apostolopoulos, "Artificial neural networks for material parameter extraction in terahertz time-domain spectroscopy," Opt. Express **30**(9), 15583–15595 (2022).
10. N. Born, D. Behringer, S. Liepelt, S. Beyer, M. Schwerdtfeger, B. Ziegenhagen, and M. Koch, "Monitoring Plant Drought Stress Response Using Terahertz Time-Domain Spectroscopy," Plant Physiol. **164**(4), 1571–1577 (2014).
11. P. Nie, F. Qu, L. Lin, T. Dong, Y. He, Y. Shao, and Y. Zhang, "Detection of Water Content in Rapeseed Leaves Using Terahertz Spectroscopy," Sensors **17**(12), 2830 (2017).
12. M. Borovkova, M. Khodzitsky, P. Demchenko, O. Cherkasova, A. Popov, and I. Meglinski, "Terahertz time-domain spectroscopy for non-invasive assessment of water content in biological samples," Biomed. Opt. Express **9**(5), 2266 (2018).
13. Y. Abautret, D. Coquillat, M. Zerrad, X. Buet, R. Bendoula, G. Soriano, N. Brouilly, D. Héran, B. Grözes-Besset, F. Chazalet, and C. Amra, "Terahertz probing of sunflower leaf multilayer organization," Opt. Express **28**(23), 35018–35037 (2020).
14. L. Gao, F. Lemarchand, and M. Lequime, "Refractive index determination of SiO2 layer in the UV/Vis/NIR range: spectrophotometric reverse engineering on single and bi-layer designs," J. Eur. Opt. Soc. - Rapid publications **8**, 13010 (2013).
15. C. Amra, M. Lequime, and M. Zerrad, *Electromagnetic Optics of Thin-Film Coatings: Light Scattering, Giant Field Enhancement, and Planar Microcavities* (Cambridge University Press, 2020).